Construction of Regulated Nanospace around a Porphyrin Core

Mutsumi Kimura,*,† Tetsuo Shiba,† Megumi Yamazaki,† Kenji Hanabusa,† Hirofusa Shirai,*,† and Nagao Kobayashi‡

Contribution from the Department of Functional Polymer Science, Faculty of Textile Science and Technology, Shinshu University, Ueda 386-8567, Japan, and Department of Chemistry, Graduate School of Science, Tohoku University, Sendai 980-8587, Japan

Received December 20, 2000

Abstract: A series of 1,3,5-phenylene-based rigid dendritic porphyrins were synthesized by Suzuki coupling between a porphyrin core and dendron units. The intramolecular energy transfer was studied by absorption and fluorescence spectroscopies. The encapsulation of the porphyrin core within the 1,3,5-phenylene dendron units was found to provide highly efficient energy transfer from the dendron units to the porphyrin core. The dendritic wedge structure affected the energy transfer efficiency. The 1,3,5-phenylene-based rigid dendron units act as highly efficient light-harvesting antennae. These dendritic porphyrins have also been examined as C_{60} hosts and substrate-selective oxidation catalysts. The attachment of the second generation of 1,3,5-phenylene-based dendron units with the porphyrin core enabled a stable inclusion of C_{60} in toluene. Furthermore, the size and shape of the nanospace in the rigid dendritic porphyrins were found to affect the selectivity of substrates in the catalytic olefin oxidations.

Introduction

Dendrimers were well-defined, three-dimensional, and nanoscopic macromolecules constructed from an interior core with a regular array of branching units.[1] When photo- and electroactive functional units are incorporated into the interior core of the dendrimers, the regular branching arrays of the dendrimers affect several functionalities through the control of the microenvironment around functional units.[2] Accordingly, the modification of functionalities with dendritic structures can possibly generate new nanoscopic materials with desirable properties.

Dendritic porphyrins have been synthesized by attaching dendrimers to porphyrins and metalloporphyrins. Aida et al. have reported dendritic effects on photochemical events and ligand bindings as dioxygen and dendritic ligands in dendritic porphyrins bearing aryl ether dendrons.[3] Diederich et al. investigated electrochemical properties of metalloporphyrins encapsulated within dendrimers.[4] They reported that dendrimers influenced the redox potentials of metalloporphyrins and sterically inhibited electron transfer from the electrode surface to the redox center. Fréchet et al. prepared the zinc porphyrin-cored dendrimers up to the forth generation and found that quenching efficiency with benzyl viologen was increased at the dendritic porphyrin possessing forth generation dendron units due to the accumulation effect of aryl ether dendrons.[5] Moore, Suslick, et al. reported regioselective and shape-selective catalytic abilities in dendritic porphyrins.[6] These dendritic porphyrins were also shown to serve as synthetic models of biological systems: light-harvesting antennas in a photosynthetic process, electron-carrying proteins, and enzymes. The molecular design of a three-dimensional dendritic structure around a porphyrin core could tune the functionalities of porphyrins and metalloporphyrins.

The focus of these previous works on dendritic porphyrins was on encapsulation in flexible dendron units. The mobility of flexible linkages in dendron units significantly affects the overall shapes of dendrimers. In contrast, rigid all-hydrocarbon dendrimers based on polyphenylene and polyphenylacetylene have also been synthesized. Moore et al. reported a convergent synthesis of rigid dendrimers based on 1,3,5-trisubstituted phenylacetylene repeating units.[7] Polyphenylene-based dendrimers have been synthesized through divergent and convergent methods as reported by Miller, Neenan, et al.,[8] Webster and Kim,[9] and Müllen et al.[10] These rigid linkages can control the mobility of dendron units, and the shapes and sizes of the rigid

† Shinshu University.

‡ Tohoku University.

(1) (a) Tomalia, D. A.; Dupont Durst, H. *Top. Curr. Chem.* **1993**, *165*, 193. (b) Newkome, G. R.; Moorefield, C. N. *Comprehensive Supramolecular Chemistry*; Pergamon: New York, 1996; Vol. 10, pp 777−832. (c) Fréchet, J. M. J. *Science* **1994**, *263*, 1710. (d) van Genderen, M. H. P.; Meijer, E. W. *Supramolecular Technology*; Wiley: New York, 1999; Chapter 2, pp 47−88.

(2) (a) Gorman, C. *Adv. Mater.* **1998**, *10*, 295. (b) Fischer, M.; Vögtle, F. *Angew. Chem., Int. Ed.* **1999**, *38*, 884. (c) Bosman, A. W.; Janssen, H. M.; Meijer, E. W. *Chem. Rev.* **1999**, *99*, 1665. (d) Newkome, G. R.; He, E.; Moorefield, C. N. *Chem. Rev.* **1999**, *99*, 1689.

(3) (a) Jin, R.-H.; Aida, T.; Inoue, S. *J. Chem. Soc., Chem. Commun.* **1993**, 1260. (b) Sadamoto, R.; Tomioka, N.; Aida, T. *J. Am. Chem. Soc.* **1996**, *118*, 3978. (c) Tomoyose, Y.; Jiang, D.-L.; Jin, R.-H.; Aida, T.; Yamashita, T.; Horie, K.; Yashima, E.; Okamoto, Y. *Macormolecules* **1996**, *29*, 5236. (d) Jiang, D.-L.; Aida, T. *Chem. Commun.* **1996**, 1523. (e) Tomioka, N.; Takasu, D.; Takahashi, T.; Aida, T. *Angew. Chem., Int. Ed.* **1998**, *37*, 1531.

(4) (a) Dandliker, P. J.; Diederich, F.; Gross, M.; Knobler, C. B.; Louati, A.; Sanford, E. M. *Angew. Chem., Int. Ed. Engl.* **1994**, *33*, 1739. (b) Dandliker, P. J.; Diederich, F.; Gisselbrecht, J.-P.; Louati, A.; Gross, M. *Angew. Chem., Int. Ed. Engl.* **1995**, *34*, 2725. (c) Weyermann, P.; Gisselbrecht, J.-P.; Boudon, C.; Diederich, F.; Gross, M. *Angew. Chem., Int. Ed.* **1999**, *38*, 3215.

(5) (a) Pollak, K. W.; Sanford, E. M.; Fréchet, J. M. J. *J. Mater. Chem.* **1998**, *8*, 519. (b) Pollak, K. W.; Leon, J. W.; Fréchet J. M. J.; Maskus, M.; Abruña, H. D. *Chem. Mater.* **1998**, *10*, 30. (c) Matos, M. S.; Hofkens, J.; De Schryver, F. C.; Hecht, S.; Pollak, K. W.; Fréchet J. M. J.; Forier, B.; Dehaen, W. *Macromolecules* **2000**, *33*, 2967.

(6) (a) Bhyrappa, P.; Young, J. K.; Moore, J. S.; Suslick, K. S. *J. Am. Chem. Soc.* **1996**, *118*, 5708. (b) Bhyrappa, P.; Vaijayanthimala, G.; Suslick, K. S. *J. Am. Chem. Soc.* **1999**, *121*, 262.

(7) (a) Xu, Z.; Kahr, M.; Walker, K. L.; Wilkins, C. L. Moore, J. S. *J. Am. Chem. Soc.* **1994**, *116*, 4537. (b) Pesak, D. J.; Moore, J. S. *Angew. Chem., Int. Ed. Engl.* **1997**, *36*, 1636. (c) Devadoss, C.; Bharathi, P.; Moore, J. S. *Macromolecules* **1998**, *31*, 8091. (d) Pesak, D. J.; Moore, J. S.; Wheat, T. E. *Macromolecules* **1997**, *30*, 6467.

10.1021/ja004312d CCC: $20.00
Published on Web 05/24/2001

Scheme 1. Synthetic Approach to a Series of Dendritic Porphyrins

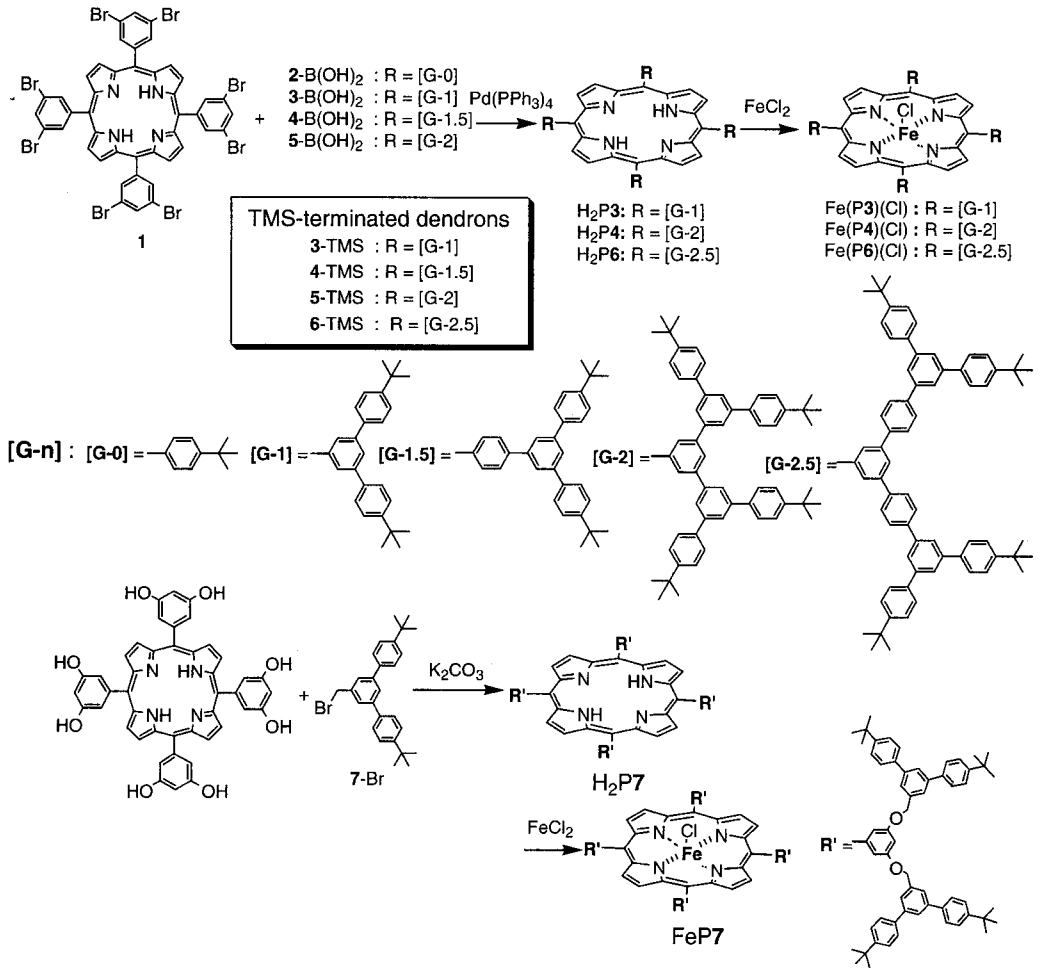

dendrimers persist in all physical environments. Such stiff and shape-persistent rigid dendrimers can create a regulated nanospace within a dendritic structure. The creation of a regulated nanospace around functional molecules might provide some unique properties, e.g., sizes, shapes, or chemical selectivities for guest molecules.

The effects of rigid dendron units on porphyrin functionalities have not been as extensively explored. Constructing a rigid dendrimer around a porphyrin core may enhance the porphyrin functionalities. Here, we describe the synthesis and characterization of a series of 1,3,5-phenylene-based dendritic porphyrins possessing a porphyrin central core. In this paper, we also discuss a structural dependence of the intramolecular singlet−singlet energy transfer from the rigid dendrons to the porphyrin core and the selective recognitions in the regulated nanospace constructed around the porphyrin core.

Results and Discussion

Synthesis of Rigid Dendritic Porphyrins. A series of 1,3,5-phenylene-based dendritic porphyrins H_2P**3**−H_2P**7** were synthesized by using the convergent methodology developed by Miller, Neenan, et al. (Scheme 1).[8] The dendron construction began by palladium-catalyzed cross coupling (Suzuki coupling) between 4-*tert*-butylphenylboronic acid and 3,5-dibromo-1-(trimethylsilyl)benzene. Purification of the first-generation **3**-TMS was accomplished by column chromatography followed by recrystallization. The trimethylsilyl group at the focal point was then converted to the corresponding boronic acid by treatment with BBr_3. Dendron **4**-$B(OH)_2$ was synthesized from **3**-$B(OH)_2$ and 4-bromo-(1-trimethylsilyl)benzene through the same procedure as that for **3**-TMS. Finally, the coupling of dendrons **2**-$B(OH)_2$, **3**-$B(OH)_2$, and **4**-$B(OH)_2$ to the porphyrin core **1** using $Pd(PPh_3)_4$ as a catalyst proceeded to yield dendritic porphyrins H_2P**3**, H_2P**4**, and H_2P**5**. The third-generation porphyrin dendrimer could not be prepared from the coupling between **1** and a higher generation of phenylboronic acid **5**-$B(OH)_2$. Matrix-assisted laser desorption/ionization time-of-flight mass spectra (MALDI-TOF-MS) of the resulting products showed a mixture of defect structures (Figure 1), suggesting that it becomes more difficult to carry out a complete coupling reaction of a focal point of a dendron unit **5**-$B(OH)_2$ with a porphyrin core. Dendritic porphyrin H_2P**7**, in which the triphenylene dendron units were linked with the porphyrin core through ether bonds, was synthesized by an alkaline-mediated coupling reaction between 5,10,15,20-tetrakis(3′,5′-dihydroxyphenyl)porphyrin[3a] and dendritic bromide **7**-Br.[11] The synthesized dendritic porphyrins were fully characterized by UV−visible spectroscopy, size-exclusion chromatography (SEC), high-performance liquid chromatography (HPLC), MALDI-TOF mass spectroscopy, and ^1H and ^{13}C NMR spectroscopy.

(8) Miller, T. M.; Neeman, T. X.; Zayas, R.; Bair, H. E. *J. Am. Chem. Soc.* **1992**, *114*, 1018.

(9) Kim, Y. H.; Webster, O. W. *J. Am. Chem. Soc.* **1990**, *112*, 4592.

(10) Berresheim, A. J.; Müller, M.; Müllen, K. *Chem. Rev.* **1999**, *99*, 1747 and related references therein.

(11) (a) Hawker, C. J.; Fréchet, J. M. J. *J. Am. Chem. Soc.* **1990**, *112*, 7638. (b) Wooley, K. L.; Hawker, C. J.; Féchet, J. M. J. *J. Am. Chem. Soc.* **1991**, *113*, 4252.

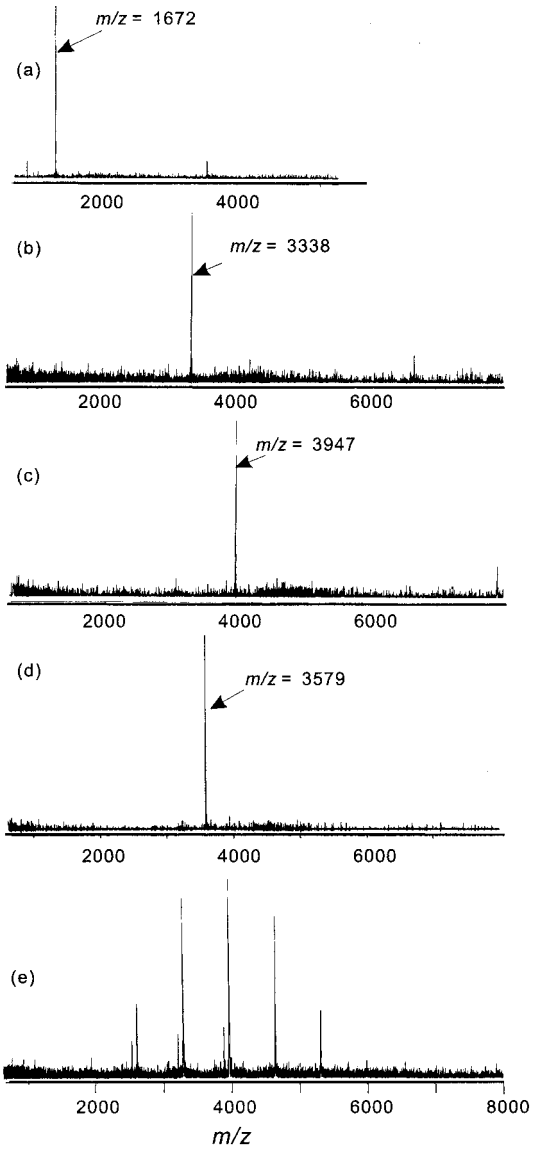

Figure 1. MALDI-TOF mass spectra of (a) H_2P**3**, (b) H_2P**4**, (c) H_2P**6**, (d) H_2P**7**, and (e) defect products after cross coupling between **1** and **5**−$B(OH)_2$.

Examinations of SEC showed that the observed molecular weight rose with each generation and that all products have sharp and symmetrical elution patterns with polydispersities (M_w/M_n) less than 1.02. With HPLC, it was possible to resolve fully substituted and partially substituted dendritic porphyrins, providing confirmation that dendron substitution in H_2P**3**, H_2P**4**, H_2P**6**, and H_2P**7** is complete. Figure 2 shows ^{1}H NMR spectra of H_2P**3**, H_2P**4**, and H_2P**6** in $CDCl_3$ at 25 °C, which provides the structural information. As shown in Figure 2, proton resonances in the aromatic region of all dendritic porphyrins are distinguishable and assignable. The proton resonances of benzene units nearer the porphyrin core shift downfield compared with those of the exterior benzene units, indicating the successive generation of a highly symmetric layered structure.

Light-Harvesting Properties of 1,3,5-Phenylene-Based Dendrons. The absorption spectra of the dendritic porphyrins H_2P**3**, H_2P**4**, H_2P**5**, and H_2P**6**, along with trimethylsilyl-terminated dendrons, were measured in CH_2Cl_2. The absorption maxima (λ_{max}) and molar extinction coefficient (ϵ) of the porphyrins are summarized in Table 1. Figure 3 illustrates the absorption spectra of the dendritic porphyrins in CH_2Cl_2. These absorption spectra are the sum of a porphyrin moiety (400−650 nm) and 1,3,5-phenylene-based dendron units (260−270 nm). The Soret bands and Q-bands of the porphyrin core remained unaltered in H_2P**3**, H_2P**4**, H_2P**6**, and H_2P**7** with different structures of the dendron units, suggesting that the electronic conditions in all dendritic porphyrins are similar to

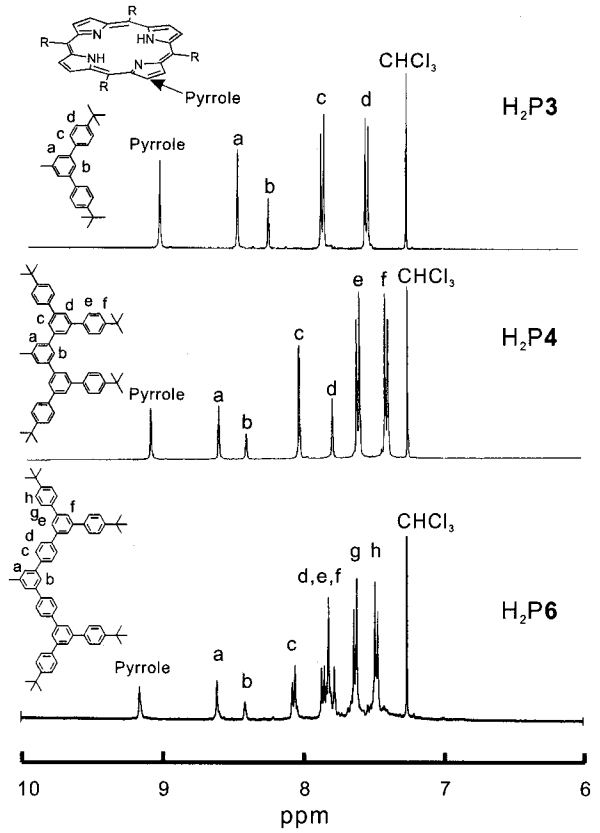

Figure 2. ^{1}H NMR spectra of dendritic porphyrins H_2P**3**, H_2P**4**, and H_2P**6** in $CDCl_3$.

Table 1. Spectroscopic and Photophysical Data for the Dendritic Porphyrins and Dendrons

	absorption,[a] λ_{max}, nm ($\log \epsilon$, M^{-1} cm^{-1})	emission,[b] λ_{max}, nm (τ, ns)	ϕ_{ET}[c]
3-TMS	262 (4.30)	354	
5-TMS	264 (4.76)	360	
6-TMS	270 (4.77)	370	
H_2P**3**	256 (4.90), 424 (5.38)	652, 719 (8.2)	0.66
H_2P**4**	262 (5.36), 424 (5.38)	651, 717 (8.3)	0.98
H_2P**6**	270 (5.37), 424 (5.38)	650, 717 (8.2)	0.74
H_2P**7**	256 (5.24), 424 (5.38)	652, 718 (8.3)	0.42

[a] In CH_2Cl_2 solution. [b] In degassed CH_2Cl_2 solution. [c] Quantum yield of energy transfer (ϕ_{ET}) in dendritic porphyrins estimated by comparing the absorption spectrum and excitation spectrum by monitoring the emission of the porphyrin moiety in degassed CH_2Cl_2.

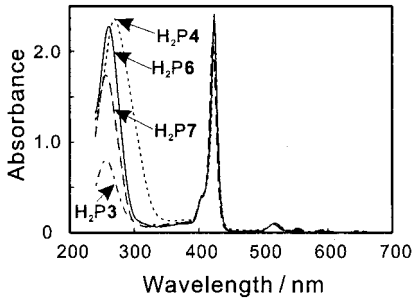

Figure 3. UV−vis absorption spectra of H_2P**3**, H_2P**4**, H_2P**6**, and H_2P**7** in CH_2Cl_2. The spectra were normalized to 5.0 μM concentration.

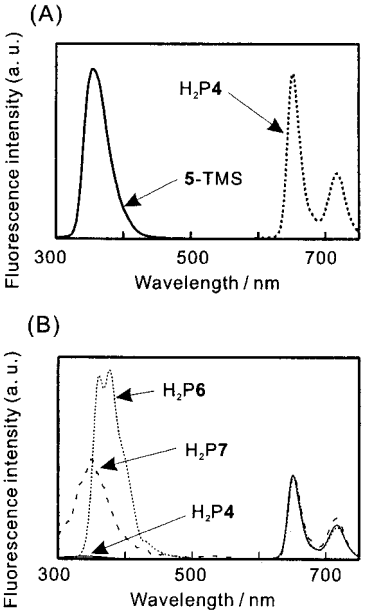

Figure 4. (A) Steady-state fluorescence spectra of **5**-TMS and H_2P**4** upon excitation at the absorption maximum of **5**-TMS (262 nm) and the Soret band of H_2P**4** (424 nm), respectively. (B) Fluorescence spectra of H_2P**4**, H_2P**6**, and H_2P**7** upon excitation at the absorption maximum of the each dendron components. The measurements were carried out in degassed CH_2Cl_2 at room temperature. All spectra are normalized to a constant absorbance at the excitation wavelength.

each other. In contrast, the absorption bands corresponding to the dendron units around 260 nm dramatically differed with the different structures of the dendron units. As the dendrimer generation increased, the ϵ value of the dendron units in the second-generation H_2P**4** nearly doubled from that of the first-generation H_2P**3**. The cross-conjugated structures of the 1,3,5-phenylene-based dendron units in H_2P**4** exhibited a strong UV absorption characteristic. The absorption intensity corresponding to the dendron units in the larger dendrimer H_2P**6**, in which a benzene spacer was inserted between the porphyrin core and the outer branching units, did not significantly change compared with that for H_2P**4**. However, the absorption band was red shifted and broadened, since H_2P**6** contained linear triphenylene units in addition to the cross conjugation of the 1,3,5-phenylene branching system. Despite the number of benzene rings being the same in H_2P**4** and H_2P**7**, the absorption intensity of the dendron units for H_2P**7** was two-thirds of that for H_2P**4**. The ether linkage in H_2P**7** led to a decrease in the electronic interaction among benzene components in the dendron units.

Figure 4A shows steady-state fluorescence spectra of H_2P**4** and trimethylsilyl-terminated dendron **5**-TMS in degassed CH_2Cl_2 upon excitation at the Soret band of the porphyrin core and λ_{max} of **5**-TMS, respectively. The fluorescence parameters for all of the dendritic porphyrins and dendrons are summarized in Table 1. The dendritic porphyrins emitted fluorescence at 650 and 717 nm and exhibited nearly the same intensities in different generations. The fluorescence of all of the dendritic porphyrins showed a normal decay profile, and the fluorescence lifetime of the porphyrin core was independent of the structural differences of the dendron units. These results suggested that the 1,3,5-phenylene-based dendritic structure hardly affected the fluorescence properties of the porphyrin core. The dendron **5**-TMS emitted strong fluorescence at 360 nm with excitation at 264 nm. By the excitation at the absorption band of 1,3,5-phenylene dendron units in H_2P**4**, the emission was mostly from the porphyrin core, and the residual fluorescence from the dendron units was very weak (Figure 4B). A mixture of the porphyrin core **1** and **5**-TMS showed no emission peaks from the porphyrin moiety with excitation at 262 nm. This result indicated the efficient intramolecular singlet−singlet energy transfer from the phenylene-based dendron units to the porphyrin core.

The efficiency of energy transfer (ϕ_{ET}) can be estimated by comparing the UV−vis spectrum and excitation spectrum of the dendron units (Table 1). When the absorption and excitation spectra are normalized at the Soret band of the porphyrin core, the ratio of the normalized excitation and absorption spectrum at λ_{max} of the dendron unit represents the total energy transfer efficiency (ϕ_{ET}). The similarity of the band shape and intensity of these two spectra for H_2P**4** indicates a high transfer efficiency. The ϕ_{ET} values in H_2P**3** and H_2P**4** were estimated to be 66 and 98%, respectively. With increasing branching layers, more photons can be harvested by the phenylene-based dendron units, and the absorbed photons are transduced to the fluorescence emission from the porphyrin core through the highly efficient energy transfer. The other dendritic porphyrins H_2P**6** and H_2P**7** exhibited a residual fluorescence in the range of 350−400 nm from the phenylene dendron units together with the fluorescence from the porphyrin core as shown in Figure 4B. Clearly, H_2P**6** and H_2P**7** have lower energy transfer efficiencies than H_2P**4**.

Recently, chromophore-containing dendrimers have attracted significant attention as artificial light-harvesting antennae due to their morphological similarities to architectures of natural light-harvesting complexes.[12] The uniform three-dimensional structures of dendrimers allow the precise placement of chromophores by the introduction of chromophores at the core, branching, and peripheral positions of the dendritic structure. There has been much work on the light-harvesting properties of the designed chromophore-containing dendrimers as dendritic polynuclear Ru and Os polypyridine complexes,[13] lanthanide-cored dendrimers,[14] rigid acceptor-terminated phenylacetylene dendrimers,[15] dendritic porphyrins,[16] and acceptor/donor dye-labeled dendrimers.[17] Among them, Jiang and Aida found that the dendritic porphyrins having a continuous array of flexible aryl ether dendron units exhibit highly efficient intramolecular energy transfer, and the energy transfer efficiency depends on the generation number and morphology of the dendritic porphyrins.[16] The intramolecular energy transfer within dendritic architectures has been explained by the Förster mechanism.[12] According to this, the energy transfer efficiency depends on the distance between donor and acceptor molecules and the spectral overlap between donor emission and acceptor absorption spectra. With increasing dendrimer size, the ϕ_{ET} value increases. The spectral overlap is better for H_2P**6** than for H_2P**4**. However, the ϕ_{ET} value in H_2P**6** is lower than that in H_2P**4**. Our attempt to apply the Förster mechanism fails to explain the highly

(12) (a) Adronov, A.; Fréchet, J. M. J. *Chem. Commun.* **2000**, 1701. (b) Stewart, G. M.; Fox, M. A. *J. Am. Chem. Soc.* **1996**, *118*, 4354. (c) Hu, Q.-S.; Pugh, V.; Sabat, M.; Pu, L. *J. Org. Chem.* **1999**, *64*, 7528. (d) Sato, T.; Jiang, D.-L.; Aida, T. *J. Am. Chem. Soc.* **1999**, *121*, 10658. (e) Li, J.; Diers, J. R.; Yang, S. I.; Bocian, D. F.; Holten, D.; Lindsey, J. S. *J. Org. Chem.* **1999**, *64*, 9090.

(13) Balzani, V.; Campagna, S.; Denti, G.; Juris, A.; Serroni, S.; Venturi, M. *Acc. Chem. Res.* **1998**, *31*, 26 and related references therein.

(14) (a) Kawa, M.; Fréchet, J. M. J. *Thin Solid Films* **1998**, *331*, 259. (b) Kawa, M.; Fréchet, J. M. J. *Chem. Mater.* **1998**, *10*, 286.

(15) Devadoss, C.; Bharathi, P.; Moore, J. S. *J. Am. Chem. Soc.* **1996**, *118*, 9635.

(16) Jiang, D.-L.; Aida, T. *J. Am. Chem. Soc.* **1998**, *120*, 10895.

(17) (a) Gilat, S. L.; Adronov, A.; Fréchet, J. M. J. *Angew. Chem., Int. Ed.* **1999**, *38*, 1422. (b) Chrisstoffels, L. A. J.; Adronov, A.; Fréchet, J. M. J. *Angew. Chem., Int. Ed.* **2000**, *39*, 2163. (c) Adronov, A.; Gilat, S. L.; Fréchet, J. M. J.; Ohta, K.; Neuwahl, F. V. R.; Fleming, G. R. *J. Am. Chem. Soc.* **2000**, *122*, 1175.

efficient energy transfer phenomena in these 1,3,5-phenylene-based dendritic porphyrins. Moreover, the decrease in the ϕ_{ET} value in H_2P**7** compared with that in H_2P**4** provided clear evidence of the presence of a through-bond pathway of energy transfer within the cross-conjugated dendritic porphyrins. A similar observation was noted in the perylene-terminated phenylacetylene dendrimers reported by Moore et al.[15] Therefore, we concluded that the high efficiency of the energy transfer from the phenylene-based dendron units to the porphyrin core can be ascribed to the efficient energy flow through the cross conjugation of the 1,3,5-phenylene dendron units (through-bond) as well as the larger overlap between the emission of the dendron units and the absorption of the porphyrin core (through-space).

Complexation of C_{60} with Rigid Dendritic Porphyrins. The inclusion of fullerenes into organic hosts through noncovalent bonds has attracted considerable interest due to the modification of fullerene functionalities as well as their purification.[18] Several organic hosts for fullerenes have been designed and synthesized.[19] Atwood et al. and Shinkai et al. discovered that *p-tert*-buthylcalix[8]arene selectively includes C_{60} in organic solvents and forms a precipitate with 1:1 stoichiometry.[20] Very recently, porphyrin dimers have also shown a selective fullerene binding with a high binding constant ($>10^5$ M^{-1}).[21] In these supramolecular hosts for fullerenes, the conformity of the C_{60} size with the host cavity enables stable complexation between the organic hosts and C_{60}.

The synthesized 1,3,5-phenylene-based dendritic porphyrins possess a regulated nanospace with different sizes. These well-defined nanospaces within the 1,3,5-phenylene-based dendrimers can provide cavities for inclusion of C_{60}. Furthermore, the porphyrin core in the dendritic porphyrins can interact strongly with C_{60} via a π-donor$-\pi$-acceptor interaction. In this context, we expect stable complexation of C_{60} with 1,3,5-phenylene-based dendritic porphyrins.

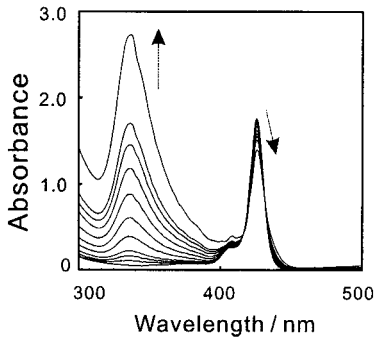

Figure 5. Effect of C_{60} concentration on the absorption spectrum of H_2P**4** in toluene at room temperature: $[H_2P\mathbf{4}] = 3.0\ \mu M$; $[C_{60}]/[H_2P\mathbf{4}] = 0, 0.33, 0.67, 1.0, 2.0, 3.3, 5.0, 6.0, 7.0, 8.3, 10.0, 16.7$.

The absorption spectrum of H_2P**4** in toluene solution changed upon the addition of C_{60}, and the Soret band was red shifted from 424 to 428 nm with decreasing absorption intensity, indicating electronic interaction between the porphyrin core within H_2P**4** and C_{60} (Figure 5). A similar spectral change was observed in the porphyrin dimers.[21] However, the other dendritic porphyrins, H_2P**3**, H_2P**6**, and H_2P**7**, showed no spectral changes in the absorption spectra after the addition of a large excess of C_{60}. We could not measure the ^{1}H and ^{13}C NMR spectra of the complex of H_2P**4** with C_{60} because of the formation of precipitate. When the equimolar toluene solution of C_{60} was admixed with the H_2P**4** solution, a red-brown precipitate was formed. Filtration of the precipitate recovered above 85% yield of the initial amount of H_2P**4** and C_{60}. Elemental analysis of the precipitate indicated a 1:1 complex of H_2P**4** and C_{60}. (Anal. Calcd for $C_{312}H_{254}N_4$: C, 92.31; H, 6.31; N, 1.38. Found: C, 92.02; H, 6.38; N, 1.37.) Furthermore, the MALDI-TOF mass spectrum of the precipitate clearly shows the mass ion peak at *m*/z 4059 corresponding to the 1:1 complex between H_2P**4** and C_{60}. The precipitate dissociated into each component after the addition of $CHCl_3$. In contrast, no precipitation was observed in the other dendritic porphyrins after the addition of C_{60}. The mixing of C_{60} with the dendritic porphyrins H_2P**3**, H_2P**6**, or H_2P**7** showed no spectral changes in the ^{1}H NMR spectra of the dendritic porphyrins and the ^{13}C NMR spectra of C_{60}. Accordingly, we judged that only H_2P**4** possessing the second generation of 1,3,5-phenylene-based dendron units can form a stable complex with C_{60}. The regulated nanospace constructed from the regulated branching system of 27 benzene rings around the porphyrin core is exactly fitted to the C_{60} size, and the multipoint interaction among the curved π surface of C_{60}, the planar π surface of the porphyrin core, and the benzene rings of the branching units work to stabilize the complex between H_2P**4** and C_{60} in toluene.

Shape-Selective Oxidation of Olefins within the Regulated Nanospace. A number of synthetic metalloporphyrins have been employed to catalyze olefin epoxidation and alkane hydroxylation with a view toward mimicking the enzymatic activity of cytochrome P-450.[22] The shape-selectivities, regioselectivities, and enantioselectivities in these catalytic reactions have also been investigated using a variety of metalloporphyrins possessing substrate recognition sites or sterically bulky substituents. The encapsulation of a metalloporphyrin core with bulky

(18) Diederich, F.; Effing, J.; Janas, U.; Jullien, L.; Plesnivy, T.; Ringsdorf, H.; Thilgen, C.; Weinsterin, D. *Angew. Chem., Int. Ed. Engl.* **1992**, *31*, 1599. Andersson, T.; Nilsson, K.; Sundahl, M.; Westman, G.; Wennerström, O. *J. Chem. Soc. Chem. Commun.* **1992**, 604. Izuoka, A.; Tachikawa, T.; Sugawara, T.; Saito, Y.; Shinohara, H. *Chem. Lett.* **1992**, 1049. Steed, J. W.; Junk, P. C.; Atwood, J. L.; Barnes, M. J.; Raston, C. L. *J. Am. Chem. Soc.* **1994**, *116*, 10346. Yoshida, Z.; Takekuma, H.; Takekuma, S.; Matsubara, Y. *Angew. Chem., Int. Ed. Engl.* **1994**, *33*, 1597. Haino, T.; Yanase, M.; Fukazawa, Y. *Angew. Chem., Int. Ed.* **1998**, *37*, 997.

(19) Covalently bonded dendrimer−fullerene and porphyrin−fullerene hybrids have been reported. (a) Dendrimer−fullerrene hybrid: Wooley, K. L.; Hawker, C. J.; Fréchet, J. M. J.; Wudl, F.; Srdanov, G.; Shi, S.; Li, C.; Kao, M. *J. Am. Chem. Soc.* **1993**, *115*, 9836. Hawker, C. J.; Wooley, K. L.; Fréchet, J. M. J. *J. Chem. Soc., Chem. Commun.* **1994**, 925. Cloutet, E.; Gnanou, Y.; Fillaut, J.-L.; Astruc, D. *Chem. Commun.* **1996**, 1565. Catalano, V. J.; Parodi, N. *Inorg. Chem.* **1997**, *36*, 537. Camps, X.; Hirsch, A. *J. Chem. Soc., Perkin Trans. 1* **1997**, 1595. Armaroli, N.; Boudon, C.; Felder, D.; Gisselbrecht, J.-P.; Gross, M.; Marconi, G.; Nicoud, J.-F.; Nierengarten, J. F.; Vicinelli, V. *Angew. Chem., Int. Ed.* **1999**, *38*, 3730. Felder, D.; Gallani, J.-L.; Guillon, D.; Heinrich, B.; Nicoud, J.-F.; Nierengarten, J.-F. *Angew. Chem., Int. Ed.* **2000**, *39*, 201. Brettreich, M.; Burghardt, S.; Böttcher, C.; Bayerl, T.; Bayerl, S.; Hirsch, A. *Angew. Chem., Int. Ed.* **2000**, *39*, 1845. (b) Porphyrin−fullerene hybrids: Imahori, H.; Hagiwara, K.; Aoki, M.; Akiyama, T.; Taniguchi, S.; Okada, T.; Shirakawa, M.; Sakata, Y. *J. Am. Chem. Soc.* **1996**, *118*, 11771. Baran, P. S.; Monaco, R. R.; Khan, A. U.; Schuster, D. I.; Wilson, S. R. *J. Am. Chem. Soc.* **1997**, *119*, 8363. Carbonera, D.; Di Valentin, M.; Corvaja, C.; Agostini, G.; Giacometti, G.; Liddell, P. A.; Kuciauskas, D.; Moore, A. L.; Moore, T. A.; Gust, D. *J. Am. Chem. Soc.* **1998**, *120*, 4398. Dietel, E.; Hirsch, A.; Zhou, J.; Riker, A. *J. Chem. Soc., Perkin Trans. 2* **1998**, 1357. Cheng, P.; Wilson, S. R.; Schuster, D. I. *Chem. Commun.* **1999**, 89.

(20) (a) Atwood, J. L.; Koutsantonis, G. A.; Raston, C. L. *Nature* **1994**, *368*, 229. (b) Suzuki, T.; Nakashima, K.; Shinkai, S. *Chem. Lett.* **1994**, 699. (c) Ikada, A.; Shinaki, S. *Chem. Rev.* **1997**, *97*, 1713.

(21) (a) Tashiro, K.; Aida, T.; Zheng, J.-Y.; Kinbara, K.; Saigo, K.; Sakamoto, S.; Yamaguchi, K. *J. Am. Chem. Soc.* **1999**, *121*, 9477. (b) Sun, D.; Tham, F. S.; Reed, C. A.; Chaker, L.; Burgess, M.; Boyd, P. D. W. *J. Am. Chem. Soc.* **2000**, *122*, 10704.

(22) (a) Cook, B. R.; Reinert, T. J.; Suslick, K. S. *J. Am. Chem. Soc.* **1986**, *108*, 7281 and related references therein. (b) Groves, J. T.; Nemo, T. E. *J. Am. Chem. Soc.* **1987**, *109*, 5045. (c) Ostovic, D.; Bruice, T. C. *J. Am. Chem. Soc.* **1989**, *111*, 6511. (d) Collman, J. P.; Brauman, J. I.; Fitzgerald, J. P.; Hampton, P. D.; Naruta, Y.; Michida, T. *Bull. Chem. Soc. Jpn.* **1988**, *61*, 47. (e) Collman, J. P.; Wang, Z.; Straumanis, A.; Quelquejeu, M.; Rose, E. *J. Am. Chem. Soc.* **1999**, *121*, 460.

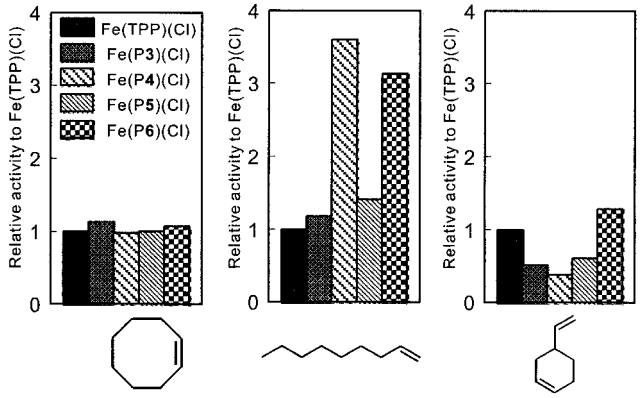

Figure 6. Epoxidation results for *cis*-cyclohexene, 1-octene, and 4-vinyl-1-cyclohexene using Fe(TPP)(Cl), Fe(P**3**)(Cl), Fe(P**4**)(Cl), Fe(P**6**)(Cl), and Fe(P**7**)(Cl) in the presence of iodosylbenzene at 25 °C. The ratios of the epoxides are normalized with respect to the corresponding Fe(TPP)(Cl) values.

polyester dendritic wedges has been found to induce regioselectivity and shape-selectivity in the catalytic reaction of olefin epoxidation.[6] The regulated nanospace around the metalloporphyrin core constructed from 1,3,5-phenylene-based dendrimers may also affect the shape selectivity in olefin epoxidation.[23]

For the preparation of dendritic iron(III) complexes, free-base H_2P**3**, H_2P**4**, H_2P**6**, and H_2P**7** were reacted with $FeCl_2$ in THF. After purification, the complete metalations in Fe(P**3**)(Cl), Fe(P**4**)(Cl), Fe(P**6**)(Cl), and Fe(P**7**)(Cl) were confirmed by UV−vis and MALDI-TOF mass spectra. It is well known that iron(III) tetraphenylporphyrin (Fe(TPP)(Cl)) forms an unreactive μ-oxo-dimer.[24] When CH_2Cl_2 solutions of dendritic porphyrins were mixed with basic aqueous solutions at pH 12.0, the MALDI-TOF mass spectra showed only a monomeric molecular ion peak, indicating no formation of μ-oxo dimers. The steric hindrance of dendritic wedges in all of the dendritic iron porphyrins was enough to prevent the formation of μ-oxo dimers.

The epoxidation of olefins with the dendritic iron porphyrins was performed in degassed CH_2Cl_2 in the presence of iodosylbenzene as the oxygen donor. Figure 6 shows results for the epoxidation of 1-octene, *cis*-cyclooctene, and 4-vinyl-1-hexene with different shapes and sizes. We can see that the rigid dendritic iron porphyrins exhibit remarkable selectivities compared with unsubstituted Fe(TPP)(Cl) and the catalytic activity strongly depends on the structures of the dendron units and substrates.[25] The catalytic activity for the epoxidation of cyclic *cis*-cyclooctene is comparable for all dendritic iron porphyrins. On the other hand, the second-generation dendrimers Fe(P**4**)(Cl) and Fe(P**7**)(Cl) show ca. 3-fold higher catalytic activity in linear 1-octene relative to Fe(TPP)(Cl) and the other dendritic iron porphyrins.

The diene 4-vinyl-1-hexene was oxidized into two products (4-vinyl-1-cyclohexene 1,2-epoxide and 4-epoxyethyl-1 cyclohexene) through the epoxidation of two different intramolecular double bonds. The total catalytic activity for the epoxidation of 4-vinyl-1-hexene decreases as the generation of dendrimers increases. While Fe(P**3**)(Cl), Fe(P**6**)(Cl), and Fe(P**7**)(Cl) show little selectivity ([4-epoxyethyl-1-cyclohexene]/[4-vinyl-1-cyclohexene 1,2-epoxide] = ca. 1.0[26]), Fe(P**4**)(Cl) exhibits regioselectivity for the epoxidation of 4-vinyl-1-cyclohexene at the least hindered double bond ([4-epoxyethyl-1-cyclohexene]/[4-vinyl-1-cyclohexene 1,2- epoxide] = 1.4[26]). The substrate selectivity was examined using the epoxidation of a 1:1 mixture of 1-octene and *cis*-cyclooctene. The high intermolecular selectivity in the epoxidation of 1-octene over that of *cis*-cyclooctene was also observed in Fe(P**4**)(Cl) ([1,2-epoxyoctane]/[cyclooctene oxide] = 2.8[26]). This observation agreed with the result reported by Suslick et al. for flexible dendritic manganese porphyrins.[6] The size and shape of the nanospace around the reaction center were found to affect the selectivity of the substrate in catalytic reactions.

Conclusion

In summary, novel rigid 1,3,5-phenylene-based dendrimers containing porphyrin and iron porphyrin complexes have been synthesized and characterized. Absorption and fluorescence spectroscopic studies demonstrated that the energy harvested by the cross-conjugated dendron units can be efficiently transferred to the porphyrin core through space and through bond. In addition, the rigid dendritic porphyrins were examined as hosts for C_{60} and shape-selective epoxidation catalysts. We found that the sizes and structures of the dendron units strongly affected the efficiency of the intramolecular energy transfer, interaction with C_{60}, and shape selectivity in the catalytic reactions of olefin epoxidation. The construction of a 1,3,5-phenylene-based regular branching array around the porphyrin core allowed the creation of a regulated nanospace within the dendrimers. The design of the nanospace could control the functionalities of the functional core. These attempts can, in principle, be applied to many nanoscopic functional materials, in which functionalities are developed by the combination of functional molecules and the designed nanospace within a single molecule.

Experimental Section

General. NMR spectra were recorded on a Bruker AVANCE 400 FT-NMR spectrometer operating at 399.65 MHz for ^{1}H in $CDCl_3$ solution. Chemical shifts are reported relative to internal TMS. IR spectra were obtained on a JASCO FS-420 spectrometer as KBr pellets. UV−vis spectra and fluorescence spectra were measured on a JASCO V-570 and a JASCO FP-750. MALDI-TOF mass spectra were obtained on a PerSeptive Biosystems Voyager-DE-Pro spectrometer with dithranol as matrix. GPC analyses were carried out with a JASCO HPLC system (pump 1580, UV detector 1575, refractive index detector 930) and a Showa Denko GPC KF-804L column (8.0 × 300 mm, polystyrene standards, M = 900−400 000 g/mol) in THF as an eluent at 35 °C (1.0 mL min^{-1}). Melting points were recorded using a Shibata MEL-270 melting point apparatus and are corrected.

Materials. All chemicals were purchased from commercial suppliers and used without purification. Solvents, such as toluene, THF, and CH_2Cl_2, were freshly distilled. Column chromatography was performed with activated alumina (Wako, 200 mesh) or Wakogel C-200. Analytical thin-layer chromatography was performed with commercial Merck plates coated with silica gel 60 F_{254} or aluminum oxide 60 F_{254}.

Porphyrin Core 1. A mixture of pyrrole (2.0 mL, 1.59 × 10^{-2} mol) and 3,5-dibromobenzaldehyde (4.2 g, 1.59 × 10^{-2} mol) in 25 mL of propionic acid was refluxed for 48 h. The residue resulting from evaporation was purified using column chromatography on activated alumina by eluting with $CHCl_3$. Yield: 11%. MALDI-TOF-MS (Dithranol): m/z = 1238 ([M + H]$^+$, 100), calcd for $C_{44}H_{22}N_4Br_8$ 1237.5.

(23) (a) Knapen, J. W. J.; van der Made, A. W.; de Wilde, J. C.; van, Leeuwen, P. W. N. M.; Wijkens, P.; Grove, D. M.; van Koten, G. *Nature* **1994**, *372*, 659. (b) Miedaner, A.; Curtis, C. J.; Barkley, R. M.; DuBois, D. L. *Inorg. Chem.* **1994**, *33*, 5482. (c) Brunner, H. *J. Organomet. Chem.* **1995**, *500*, 39. (d) Chow, H.-F.; Mak, C. C. *J. Org. Chem.* **1997**, *62*, 5116. (e) Kimura, M.; Sugihara, Y.; Muto, T.; Hanabusa, K.; Shirai, H.; Kobayashi, N. *Chem. Eur. J.* **1999**, *5*, 3495.

(24) Cheng, B.; Hobbs, J. D.; Debrunner, P. G.; Erlebacher, J.; Shelnutt, H. A.; Scheidt, W. R. *Inorg. Chem.* **1995**, *34*, 102.

(25) During catalytic reaction, less than 10% degradation of dendritic porphyrins had occurred as analyzed by UV−vis spectral change.

(26) The distribution of epoxide products for 4-vinyl-1-hexene and the ratio of the epoxide products for 1-octene and *cis*-cyclooctene are normalized with respect to the value for nondendritic Fe(TPP)(Cl).

3-TMS. Yield: 93%. ^{1}H NMR ($CDCl_3$, 400 MHz): $\delta = 7.76$ (2H, s, Ph), 7.67 (1H, s, Ph), 7.57 (4H, d, $J = 8.1$ Hz, Ph), 7.47 (4H, d, $J = 8.3$ Hz, Ph), 1.37 (18H, s, $-C(CH_3)_3$), 0.33−0.34 (9H, s, $-Si(CH_3)_3$).

4-TMS. Synthesized from **3**-$B(OH)_2$ and 4-bromo-1-(trimethylsilyl)-benzene. Yield: 82%. ^{1}H NMR ($CDCl_3$, 400 MHz): $\delta = 7.77$ (1H, s, Ph), 7.75(2H, s, Ph), 7.67 (2H, d, $J = 8.1$ Hz, Ph), 7.63 (2H, d, $J = 8.3$ Hz, Ph), 7.59 (4H, d, $J = 8.3$ Hz, Ph), 7.49 (4H, d, $J = 8.3$ Hz, Ph), 1.38 (18H, s, $-C(CH_3)_3$), 0.31 (9H, s, $-Si(CH_3)_3$). MALDI-TOF-MS (Dithranol): $m/z = 489$ ($[M + H]^+$, 100), calcd for $C_{35}H_{42}Si$ 490.

5-TMS. Synthesized from **3**-$B(OH)_2$ and 3,5-dibromo-1-(trimethylsilyl)benzene. Yield: 74%. ^{1}H NMR ($CDCl_3$, 400 MHz): $\delta = 7.92$ (1H, s, Ph), 7.79 (8H, m, Ph), 7.63 (8H, d, $J = 8.1$ Hz, Ph), 7.49 (8H, d, $J = 8.4$ Hz, Ph), 1.48 (36H, s, $-C(CH_3)_3$), 0.33−0.34 (9H, s, $-Si-(CH_3)_3$). MALDI-TOF-MS (Dithranol): $m/z = 830$ ($[M + H]^+$, 100), calcd for $C_{61}H_{70}Si$ 831.

1,3,5-Phenylene-Based Dendritic Porphyrin H_2P3. A Schlenk flask was charged with **1** (0.18 g, 4.32×10^{-4} mol) and $Pd(PPh_3)_4$ (0.03 g, 2.60×10^{-5} mol) under an Ar atmosphere. Solutions of **2**-$B(OH)_2$ (1.35 g, 1.44×10^{-3} mol) in THF (6 mL) and Na_2CO_3 (2.0 M, 7 mL) in H_2O were prepared and deoxygenated with a stream of Ar. These solutions and deoxygenated toluene were added to the reaction vessel, and the mixture was refluxed under Ar for 72 h. The reaction mixture was poured into a mixture of H_2O and diethyl ether. The aqueous phase was washed with ether, and the organic phases were combined and washed with 1 M NaOH aqueous solution and brine. The crude product was purified using column chromatography on activated alumina by eluting with CH_2Cl_2/*n*-hexane (1:9 v/v), and the resulting material was recrystallized from 2-methoxyethanol. Yield: 57%. ^{1}H NMR ($CDCl_3$, 400 MHz): $\delta = 9.04$ (8H, s, pyrrole), 8.48 (8H, s, Ph), 8.25 (4H, s, Ph), 7.86 (16H, d, $J = 8.2$ Hz, Ph), 7.54 (16H, d, $J = 8.3$ Hz, Ph), 1.37 (36H, s, $-C(CH_3)_3$), −2.58 (2H, s, −N*H*). MALDI-TOF-MS (Dithranol): $m/z = 1672$ ($[M + H]^+$, 100), calcd for $C_{124}H_{126}N_4$ 1670.9.

The synthetic procedure for H_2P**4** and H_2P**5** is similar to that for H_2P**3**.

H_2P4. Prepared from **1** and **3**-$B(OH)_2$ and purified by column chromatography (activated alumina, CH_2Cl_2/*n*-hexane (1:9 v/v)) and recrystallization from 2-methoxyethanol. Yield: 24%. ^{1}H NMR ($CDCl_3$, 400 MHz): $\delta = 9.11$ (8H, s, pyrrole), 8.62 (8H, s, Ph), 8.42 (4H, s, Ph), 8.03 (16H, s, Ph), 7.80 (8H, s, Ph), 7.61 (32H, d, $J = 8.3$ Hz, Ph), 7.40 (32H, d, $J = 8.3$ Hz, Ph), 1.37 (144H, s, $-C(CH_3)_3$), −2.58 (2H, s, −N*H*). ^{13}C NMR ($CDCl_3$): $\delta = 150.5$, 142.7, 142.4, 142.0, 141.7, 140.6, 138.3,132.5, 129.1, 127.1, 126.9, 125.7, 125.4, 125.2, 34.5, 31.3. MALDI-TOF-MS (Dithranol): $m/z = 3337$ ($[M + H]^+$, 100). Anal. Calcd for $C_{252}H_{254}N_4$: C, 90.65; H, 7.67; N, 1.68. Found: C, 90.70; H, 7.65; N, 1.66.

H_2P5. Prepared from **1** and **4**-$B(OH)_2$ and purified by column chromatography (activated alumina, CH_2Cl_2/*n*-hexane (1:9 v/v)) and recrystallization from 2-methoxyethanol. Yield: 11%. ^{1}H NMR ($CDCl_3$, 400 MHz): $\delta = 9.15$ (8H, s, pyrrole), 8.60 (8H, s, Ph), 8.40 (4H, s, Ph), 8.05 (16H, m, Ph), 7.76−7.86 (40H, m, Ph), 7.64 (32H, d, $J = 8.3$ Hz, Ph), 7.45 (32H, d, $J = 8.3$ Hz, Ph), 1.48 (144H, s, $-C(CH_3)_3$), −2.57 (2H, s, −N*H*). MALDI-TOF-MS (Dithranol): $m/z = 3947$ ($[M + H]^+$, 100), calcd for $C_{300}H_{286}N_4$ 3947.

Partially Flexible Dendritic Porphyrin H_2P7. The dendritic bromide **7**-Br was synthesized from 3,5-dibromobenzoic acid methyl ester and 4-*tert*-butylphenylboronic acid. Cross coupling between 3,5-dibromobenzoic acid methyl ester and 4-*tert*-butylphenylboronic acid in the presence of $Pd(PPh_3)_4$ (**7**-$COOCH_3$), reduction of methyl ester (**7**-OH), and bromination with CBr_4 and triphenylphosphine gave the dendritic bromide **7**-Br.[11]

7-$COOCH_3$. The synthetic procedure for **7**-$COOCH_3$ is similar to that for **3**-TMS. Yield: 95%. FT-IR (KBr): 1720 cm^{-1}. ^{1}H NMR ($CDCl_3$, 400 MHz): $\delta = 8.22$ (2H, s, Ph), 7.98 (1H, s, Ph), 7.60 (4H, d, $J = 8.4$ Hz, Ph), 7.48 (4H, d, $J = 8.3$ Hz, Ph), 3.96 (3H, s, $COOCH_3$), 1.41 (18H, s, $-C(CH_3)_3$).

7-OH. To a stirred suspension of lithium aluminum hydride (0.25 g, 6.20×10^{-3} mol) in dry THF (30 mL) was added a solution of **7**-$COOCH_3$ (1.24 g, 3.1×10^{-3} mol) in dry THF (10 mL) dropwise under nitrogen. After addition was complete, the reaction mixture was stirred for 2 h at room temperature. Water (2 mL) and 1.0 M NaOH aqueous solution (2 mL) were added to the reaction mixture. The mixture was filtered, and the filtrate was evaporated to dryness. The crude product was purified by column chromatography (silica gel, eluting with *n*-hexane gradually increasing to CH_2Cl_2/*n*-hexane (9:1 v/v)). Yield: 95%. FT-IR (KBr): disappearance of peak at 1720 cm^{-1}. ^{1}H NMR ($CDCl_3$, 400 MHz): $\delta = 7.72$ (1H, s, Ph), 7.53 (6H, m, Ph), 7.45 (4H, d, $J = 8.3$ Hz, Ph), 4.73 (2H, s, CH_2OH), 1.52 (18H, s, $-C(CH_3)_3$).

7-Br. To a solution of **7**-OH (1.00 g, 2.68×10^{-3} mol) in 5.0 mL dry THF were added CBr_4 (2.22 g, 6.70×10^{-3} mol) and triphenylphosphine (1.75 g, 6.70×10^{-3} mol) with stirring for 15 min at room temperature. The reaction mixture was poured into a mixture of H_2O and CH_2Cl_2. The aqueous phase was washed with CH_2Cl_2, and the organic phases were combined and evaporated to dryness. The crude product was purified using column chromatography (silica gel, eluting with *n*-hexane gradually increasing to CH_2Cl_2/*n*-hexane (1:2 v/v)). Yield: 78%. ^{1}H NMR ($CDCl_3$, 400 MHz): $\delta = 7.71$ (1H, s, Ph), 7.55 (6H, m, Ph), 7.46 (4H, d, $J = 8.3$ Hz, Ph), 4.53 (2H, s, CH_2Br), 1.52 (18H, s, $-C(CH_3)_3$).

H_2P7. 5,10,15,20-Tetrakis(3′,5′-dihydroxyphenyl)porphyrin (32.8 mg, 4.59×10^{-5}mol) and **7**-Br (0.20 g, 4.59×10^{-4} mol) were dissolved in acetone (10 mL) containing K_2CO_3 (0.10 g) and 18-crown-6 (catalytic amount), and the reaction mixture was refluxed for 5 days with stirring. The mixture was filtered, and the filtrate was evaporated to dryness. The crude product was purified by column chromatography (activated alumina, eluting with *n*-hexane gradually increasing to CH_2Cl_2). Yield: 32%. ^{1}H NMR ($CDCl_3$, 400 MHz): $\delta = 8.91$ (8H, s, pyrrole), 7.73 (8H, s, Ph), 7.66 (16H, s, Ph), 7.56 (32H, d, $J = 8.4$ Hz, Ph), 7.36 (32H, d, $J = 8.1$ Hz, Ph), 5.31 (16H, m, $-CH_2O-$), 1.48 (144H, s, $-C(CH_3)_3$), −2.53 (2H, s, −N*H*). MALDI-TOF-MS (Dithranol): $m/z = 3579$ ($[M + H]^+$, 100), calcd for $C_{260}H_{270}N_4Cl$ 3578.

Dendritic Iron Porphyrin Fe(H_2P3)(Cl). $FeCl_2$ (10.0 mg, 7.89×10^{-5} mol) and H_2P**3** (30.0 mg, 1.79×10^{-5} mol) were dissolved in 20 mL of THF, and the reaction mixture was refluxed under Ar. During the reaction, the UV−vis spectrum of the reaction mixture was monitored. The mixture was refluxed until no change in the Soret band was observed. The resulting iron complex was purified by column chromatography (activated alumina, CH_2Cl_2) and treatment with methanoic HCl. Yield: 59%. UV−vis (CH_2Cl_2): λ_{max} (log ϵ) = 424 (5.04), 258 (5.16). MALDI-TOF-MS (Dithranol): $m/z = 1725$ ([M − Cl]), calcd for $C_{124}H_{124}N_4FeCl$ 1761.

The synthetic procedure for Fe(H_2P**4**)(Cl), Fe(H_2P**5**)(Cl), and Fe-(H_2P**6**)(Cl) is similar to that for Fe(H_2P**3**)(Cl).

Fe(H_2P4)(Cl). Yield: 76%. UV−vis (CH_2Cl_2): λ_{max} (log ϵ) = 424 (5.04), 260 (5.37). MALDI-TOF-MS (Dithranol): $m/z = 3391$ ([M − Cl]), calcd for $C_{252}H_{254}N_4FeCl$ 3427.

Fe(H_2P5)(Cl). Yield: 68%. UV−vis (CH_2Cl_2): λ_{max} (log ϵ) = 424 (5.04), 270 (5.37). MALDI-TOF-MS (Dithranol): $m/z = 4000$ ([M − Cl]), calcd for $C_{300}H_{284}N_4FeCl$ 4036.

Fe(H_2P6)(Cl). Yield: 88%. UV−vis (CH_2Cl_2): λ_{max} (log ϵ) = 424 (5.04), 258 (5.24). MALDI-TOF-MS (Dithranol): $m/z = 3634$ ([M − Cl]), calcd for $C_{260}H_{268}O_8N_4FeCl$ 3668.

Catalytic Reactions. Epoxidations of alkenes were performed in degassed CH_2Cl_2 using iodosylbenzene as an oxygen atom transfer reagent. A solution of iodosylbenzene (10.0 μmol) in CH_2Cl_2 was added to the mixed solution of alkene (500.0 μmol) and iron complex (1.0 μmol). After addition, the mixture was stirred at 25 °C under Ar for 30 min. After 30 min, the internal standard (*n*-decane) was added to the reaction mixture, and all oxidation products were identified by GC, GC−MS, and ^{1}H NMR. Standard epoxides were purchased from commercial chemical suppliers. The yields of the oxidation products were determined by GC using the internal standard method. No reaction occurred in the absence of the catalysts in the reaction examined under the same experimental conditions.

Acknowledgment. This research was partially supported by a Grant-in-Aid for COE Research "Advanced Fiber/Textile Science and Technology" (No. 10CE2003) and Scientific Research (No. 11450366) from the Ministry of Education, Science, Sports, and Culture of Japan.

JA004312D